Green open access: versione post print conforme all'originale accettata
https://pubs.acs.org/doi/10.1021/acs.molpharmaceut.0c00396
DOI: 10.1021/acs.molpharmaceut.0c00396

Fine-Tuning the Interaction and Therapeutic Effect of Cu(II) Carbosilane Metallodendrimers in Cancer Cells: An In Vitro Electron Paramagnetic Resonance Study

Barbara Canonico[a]*, Riccardo Carloni[b], Natalia Sanz del Olmo[c], Stefano Papa[a], Maria Gemma Nasoni[a], Alberto Fattori[b], Michela Cangiotti[b], F. Javier de la Mata[c,d,e], Maria Francesca Ottaviani[b], and Sandra García-Gallego[c,d,e]*

[a] Department of Biomolecular Science (DiSB), University of Urbino "Carlo Bo", Urbino, Italy.
[b] Department of Pure and Applied Sciences, University of Urbino "Carlo Bo", Urbino, Italy.
[c] Department of Organic and Inorganic Chemistry, and Research Institute in Chemistry "Andrés M. del Río" (IQAR), University of Alcalá, Madrid, Spain.
[d] Networking Research Center on Bioengineering, Biomaterials and Nanomedicine (CIBER-BBN), Spain.
[e] Institute Ramón y Cajal for Health Research (IRYCIS).
* Corresponding authors.

Abstract

Copper(II) carbosilane metallodendrimers are promising nanosized anticancer metallodrugs. The precise control on their design enables an accurate structure-to-activity study. We hypothesized that different structural features, such as the dendrimer generation and metal counterion, modulate the interaction with tumor cells, and subsequently, the effectivity and selectivity of the therapy. A computer-aided analysis of the electron paramagnetic resonance (EPR) spectra allowed us to obtain dynamical and structural details on the interactions over time between the dendrimers and the cells, the myeloid U937 tumor cells and peripheral blood mononuclear cells (PBMC). The intracellular fate of the metallodendrimers was studied through a complete *in vitro* evaluation, including cytotoxicity, cytostaticity, and sublethal effects regarding mitochondria function, lysosomal compartments, and autophagic organelle involvement. EPR results confirmed a higher membrane stabilization for chloride dendrimers and low generation complexes, which ultimately influence the metallodrug uptake and intracellular fate. The *in vitro* evaluation revealed that Cu(II) metallodendrimers are cytostatic and moderate cytotoxic agents for U937 tumor cells, inducing death processes through the mitochondria–lysosome axis as well as autophagic vacuole formation, while barely affecting healthy monocytes. The study provided valuable insight into the mechanism of action of these nanosized metallodrugs and relevant structural parameters affecting the activity.

KEYWORDS: metallodendrimer, copper, cancer cell, EPR, interaction

1. Introduction

Cancer is a multifactorial disease with an alarming incidence worldwide, accounting for 18.1 million new cases and 9.6 million deaths in 2018. (1) According to the World Health Organization, the global cancer burden keeps rising due to different factors, such as population growth and aging, or the prevalence of certain causes of cancer linked to social and economic development. (2) The complexity of this disease is related to the unique fingerprint in each tumor, which hinders the development of a universal therapeutic approach. Furthermore,

current treatments present serious drawbacks, including the development of drug resistance and the severe side effects, due to the lack of selectivity to tumor tissues. Overall, these reasons are continuously fueling the development of new antitumor strategies.

Cancer nanotechnology is currently an established field of research, providing unique approaches for the early diagnosis, prevention, or personalized therapy of cancer. (3,4) The success of this strategy, compared to traditional cancer therapeutics, is based on two main properties: (i) the nanometric size of the nanoparticles (NPs) enables a preferential accumulation in solid tumors through the enhanced permeability and retention effect, thus bypassing traditional drug resistance mechanisms; (ii) the large surface area of the NPs is available for conjugating a large therapeutic payload of a single drug or multiple drugs, targeting moieties or diagnostic agents. Primarily, the design of safe and efficient nanomedicines requires a thorough understanding of uptake and trafficking within the cell. While most nanoparticles employ endocytic pathways to enter the cells, the interaction with biological membranes (5)depends on the physicochemical features of the NPs, size, shape, surface properties, and, on cellular parameters, the phase of the cycle or the type of cell. After internalization, NPs first encounter the early endosomes, membrane-bound intracellular vesicles that carry the cargo to the target cellular destination. However, NPs can also enter two different degradation routes: (1) the endolysosomal pathway, where the early endosomes mature to late endosomes and then integrate with lysosomes capable of degrading the trapped NPs; (2) the autophagosome pathway, where cytoplasmic contents are surrounded by the autophagosome and delivered to the lysosome for degradation. Thus, the particular characteristics of the nanoparticle will dictate its biological fate.

Dendrimers are the ultimate precision NPs with promising potential in many different biomedical applications, including cancer. (6−8) Their monodispersed and highly branched structure enables on-demand and controlled attachment of anticancer drugs, tumor-targeting moieties, diagnostic agents, or even a combination of them into the so-called theranostic nanoparticles. (9,10) Unlike other types of nanoparticles, the accurate control on the dendrimer synthesis provides ideal testbeds for studying the influence of the different structural parameters on the biological activity. Multiple studies have focused on revealing dendrimers mode of action, analyzing their interaction with membranes and cells (11,12) as well as their cell uptake and internal trafficking. (13,14) For example, cationic dendrimers are generally internalized into the cells through endocytosis. As a result, they can suffer endosomal escape and interact with different organelles, affect cellular processes, and induce apoptotic cell death. (15−17)Nevertheless, important differences arise depending on the nature of the dendritic scaffold. For example, cationic poly(amidoamine) (PAMAM) and poly(propylenimine) (PPI) dendrimers induced apoptosis in murine neural cells, (18,19) while cationic phosphorus dendrimers induced necrosis, (20) considering the much higher number of positive charges at the surface for the same generation. Cationic carbosilane dendrimers, comprising a more hydrophobic scaffold, have shown an enhanced interaction with cell membranes, altering the membrane fluidity. (21)The presence of metal complexes at the surface of carbosilane dendrimers can further tune their interaction with cell membranes, as previously observed with copper(II) and ruthenium(II) complexes. (22) Previous studies from our group have shown that nanosized metallodrugs can avoid the drawbacks of antitumor therapies. (23) In particular, copper(II) carbosilane dendrimers are promising antitumor agents considering the following: (i) the high stability provided by the chelating iminopyridine ligands and the carbosilane scaffold, (ii) the water solubility, (iii) the structure perfection of the dendritic molecule, which enables an exceptional structure-to-property relationship, (iv) the unique interaction with cell membranes, tunable through the dendrimer generation and the Cu(II) counterion.

Nevertheless, the mechanism of action of these metallodrugs has not been disclosed nor the uptake in cells. Preliminary studies, using CTAB micelles and lecithin liposomes as model cell membranes, (22) provided relevant information on the interacting ability between the dendrimers and the membranes. However, these are simplified models that cannot match the living cell complexity and, importantly, the differences between healthy and tumor cells.

In order to confirm the validity of the previous results in a practical setting and gain insight into the mode of action of the complexes, cell lines were used in the present study. The interactions occurring between Cu(II) metallodendrimers and healthy or tumor cells were investigated in the function of the incubation time, by deeply analyzing electron paramagnetic resonance (EPR) spectra, as well as through *in vitro* experiments. The EPR study provided dynamical and structural information on the *in vitro* behavior of the metallodendrimers in both healthy and tumor cells. This technique has already demonstrated to be a powerful tool to characterize Cu(II) dendrimer complexes. (12,22−25) Finally, the intracellular trafficking and mechanism of action of the Cu(II) carbosilane dendrimer complexes to be used as anticancer drugs was evaluated by means of various biological tests, including cytotoxicity, alteration of mitochondria membrane potential, and autophagy flux.

2. Methods

2.1. Cu(II) Complexes and Metallodendrimers

In this study, two families of copper(II) carbosilane complexes, bearing nitrate (**1**–**3**) and chloride (**4**–**6**) ligands (Figure 1), were selected with the purpose of studying the influence of the metal counterion and the generation on their antitumor activity. The Cu(II) mononuclear complexes and first- and second-generation metallodendrimers were synthesized as previously described. (22,23) Unless otherwise specified, the reagents used for the sample preparations were purchased from Sigma-Aldrich (St. Louis, MO, USA) and used without any further manipulation.

Figure 1

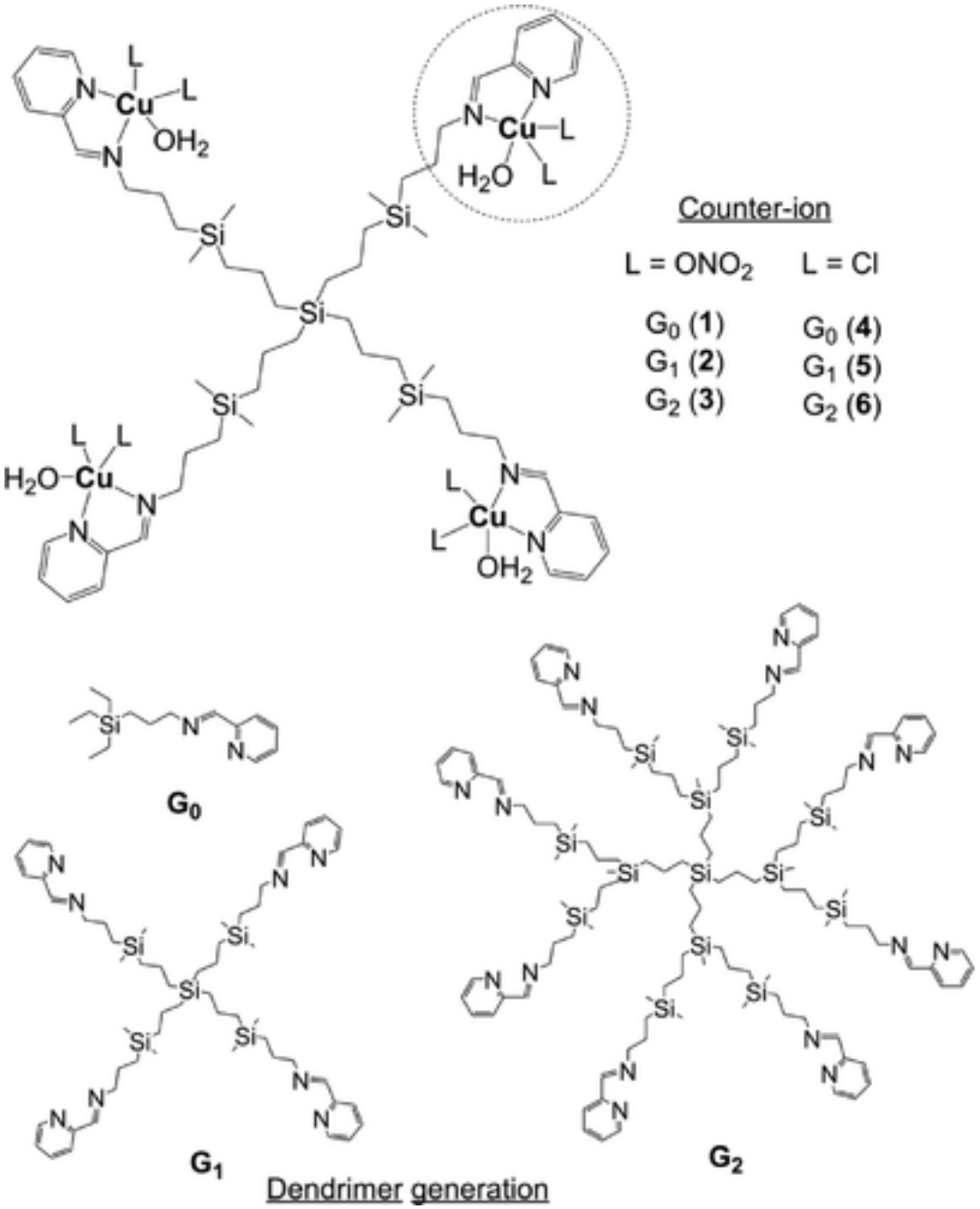

Figure 1. Structure of the carbosilane metallodendrimers **1**–**6** used in this work, highlighting the parameters studied.

2.2. Cell Lines and Primary Cultures

Human PBMCs (peripheral blood mononuclear cells) were isolated from buffy coats of anonymized donors obtained from the Transfusion Center of Urbino Hospital. No specific approval from an institutional review board was required considering that (1) no personal patient information was made available; (2) buffy coats could not be used for the treatment of patients and were waste products for the blood transfusion center; (3) blood donors were verbally informed that parts of the donation that cannot be used for patient treatment may be used for scientific research. PBMCs were isolated from buffy coats through density gradient separation using Lymphoprep solution (specific density, 1.077; Axis-Shield PoC AS, Oslo, Norway). Cells were washed twice in phosphate buffer saline (PBS) by centrifugation at 400*g* and suspended in RPMI-1640 with 10% (v/v) heat-inactivated fetal bovine serum (FBS), 100 µg/mL penicillin, 100 µg/mL streptomycin, and 2 mM l-glutamine.

The U937 cell line (Sigma-Aldrich, USA) was grown in the RPMI-1640 medium supplemented with 10% (v/v) heat-inactivated FBS, 100 U/mL penicillin, 100 µg/mL streptomycin, and 2 mM l-glutamine, at 37 °C in humidified air with 5% CO_2.

2.3. Electron Paramagnetic Resonance

Metallodendrimers solutions (1 mM concentration in surface groups in RPMI buffer) were added to 12-well plates containing RPMI with and without cells (5×10^5 cells/mL) and subsequently analyzed by EPR; to exclude an effect of the cell amount, higher and lower cell concentrations were also analyzed. The incubation times ranged from 0 to 72 h. All EPR experiments were performed at 37 °C.

EPR spectra were acquired using an EMX spectrometer (Bruker) operating at X band (9.5 GHz) and interfaced with a PC (a Bruker software was used for handling and analyzing the EPR spectra). The temperature was controlled with a Bruker ST3000 variable-temperature assembly.

Analysis of EPR Spectra of Cu(II) Metallodendrimers in RPMI in the Absence and Presence of the Cells

The EPR spectra of Cu(II) metallodendrimers were constituted by two components, which were termed “fast” and “slow” on the basis of their line shapes. The relative percentages of the components were obtained by subtracting spectra containing these components in different ratios from each other. Afterward, the extracted components and the overall spectra were doubly integrated to calculate the relative percentage of each component. Then, the well-known calculation method of Budil et al. (26) was used to compute the components and obtain the following main parameters: (a) the g_{ii} main components of the g tensor for the coupling between the unpaired electron spin and the magnetic field and A_{ii} main components of the A tensor for the coupling between the electron spin and the copper nuclear spin. For an axial symmetry, where g_{zz} and A_{zz} are the largest values, the z molecular axis corresponds to the main direction of the orbital containing the unpaired electron. The magnetic g_{ii} and A_{ii}components were compared with values found in previous literature in order to extract information about (12,22−25,27−33) (i) the type of coordination in Cu(II) complexes (such as the number of oxygen and nitrogen ligands); (ii) the geometry of the Cu(II) complex; and (iii) the strength of the coordinating bonds. In detail, an increase in the A_{ii} values (mainly A_{zz}, but, for clarity, the average value $\langle A \rangle = (A_{xx} + A_{yy} + A_{zz})/3$ was calculated and compared between spectra) and a decrease in the g_{ii} values (mainly g_{xx} was clearly evaluable in all our spectra) are usually reflected in an increased number of nitrogen ligands and/or by a stronger interaction; (b) the correlation time for the rotational motion (τ) that provides information about the flexibility and coordination strength of the dendrimer branches by measuring the mobility of the complex; an increase of τ reveals an increase of the microviscosity at the Cu(II) site and, consequently, a decreased in mobility.

2.4. *In Vitro* Cytotoxicity Assays

Cytotoxicity (absolute count and cell death) was evaluated through flow cytometry. U937 and PBMCs were seeded at a density of 10^6 cells/well in 12-well plates with 1 mL/well of medium to which 1 mL of metallodendrimer was added at a final concentration of 10^{-5} M and incubated for 24, 48, and 72 h at 37 °C in a 5% CO_2 humidified air. Therefore, the solutions for biological tests contained 100 times diluted metallodendrimer when compared to the solutions for EPR experiments. Despite the disadvantage created by the sensitivity limit of the EPR technique, which needs a relatively high concentration of paramagnetic species, this technique provides *in situ* information on the interactions occurring between the dendrimers and the cells. This information did not suffer from concentration variation as demonstrated by the invariability of the EPR spectra relative to the cell concentration.

To evaluate cell death features, cells were incubated with propidium iodide (PI, 50 µg/mL, Sigma-Aldrich) for 30 min; the PI^{dim} and PI^{bright} clusters were then studied, which detected apoptotic and necrotic cells, respectively. To perform absolute cell counting, 100 µL of the sample was carefully dispensed at the bottom of the tube and incubated with Dako CytoCount beads (50 µL, Dako Denmark A/S). Within 60 min, samples were acquired with a FACSCantoII cytometer (Becton Dickinson, BD, USA). Approximately 20 000 cell events were collected. Set-up and calibration procedures were optimized for the absolute counting protocols.

2.5. Determination of Mitochondrial Potential ($\Delta\Psi_m$)

Changes in mitochondria membrane potential were investigated through staining with tetramethylrhodamine ethyl ester perchlorate (TMRE, Sigma-Aldrich). TMRE is a $\Delta\Psi_m$-specific dye able to selectively enter into mitochondria, producing red fluorescence. TMRE (40 nM) was added to the sample and, after 15 min of incubation, fluorescence was measured by flow cytometry.

2.6. Detection of Acidic Organelles

To detect the acidification of the subcellular compartments, samples were labeled with 100 nM LysoTracker Green dye (Molecular Probes) for 10 min at 37 °C, and then the fluorescence intensity was measured by flow cytometry. LysoTracker probes are fluorescent acidotropic probes for labeling and tracking acidic organelles in live cells.

2.7. Autophagy Detection

After dendrimer treatment, the cells were incubated with 50 µM monodansylcadaverine (MDC, Sigma-Aldrich) at 37 °C for 10 min and then analyzed by flow cytometry. MDC is an autofluorescent dye that accumulates in autophagic-involved vacuoles (AIVs) due to a combination of ion trapping and specific interactions with membrane lipids.

2.8. Cytometric Analyses

Cytometry assays were carried out with a FACSCanto II flow cytometer (BD, Biosciences) equipped with an argon laser (Blue, Ex 488 nm), a helium–neon laser (Red, Ex 633 nm), and a solid-state diode laser (Violet, Ex 405 nm). Analyses were performed with FACSDiva software (BD); approximately 10 000 cell events were acquired for each sample.

2.9. Statistical Analyses

Data are shown as the mean ± standard deviation (SD) of at least three independent experiments. Analyses of variance (ANOVA) approaches were used to compare values between more than two different experimental groups for data that met the normality assumption. Two-way ANOVA was followed by a Bonferroni posthoc test. *P* values less than 0.05 were considered statistically significant. All statistical analyses were done using GraphPad Prism 5.0 (GraphPad software, U.S.A).

3. Results and Discussion

In our previous studies, (22) copper(II) carbosilane dendrimers (Figure 1) demonstrated an extraordinary interacting ability toward model cell membranes, i.e., CTAB micelles and lecithin liposomes.

EPR analysis indicated that higher generation dendrimers and chloride-containing systems exhibited an increase in the relative amount and strength of the interaction between the Cu(II) ions within the dendrimer in the presence of the model membranes. Interestingly, the stabilization of the Cu(II) complexes at the membrane level reduced the toxicity toward cancer cells. Aiming to unveil the mechanism of action of these metallodendrimers in viable cells, their interaction with the healthy cell line PBMC and the tumor cell line U937 was evaluated using computer-aided EPR and a wide range of well-validated tests for biological assays.

3.1. EPR Analysis of Cu(II) Metallodendrimers in the Absence and Presence of Cells

EPR enabled the evaluation of the dendrimers' behavior in the absence and presence of selected cell lines, namely, the healthy cell line PBMC and the tumor cell line U937, at different incubation times ranging from 0 to 72 h. Unlike former studies in model membranes using PBS, (22) this study was performed using the RPMI medium. The spectra of the dendrimers alone in RPMI showed two components, which were termed "fast" and "slow" on the basis of the different resolution of the magnetic components for the g and A tensors. This is represented in Figure 2A for G_1-(ONO_2) (**2**). Instead, three components have been found for the same dendrimers in PBS. (22) The change from PBS to RPMI media produced the disappearance of the component termed "component O" observed in PBS, arising from a Cu(II)-O_4 coordination (Cu(II) binding with 4 oxygen sites, which may be water or phosphate groups). This is probably due to the presence of amino groups in the RPMI medium, which preferentially bind Cu(II) ions. Amino groups are present in several components of the RPMI medium, like vitamins (for instance, vitamin B12), glutathione, and biotin.

Figure 2

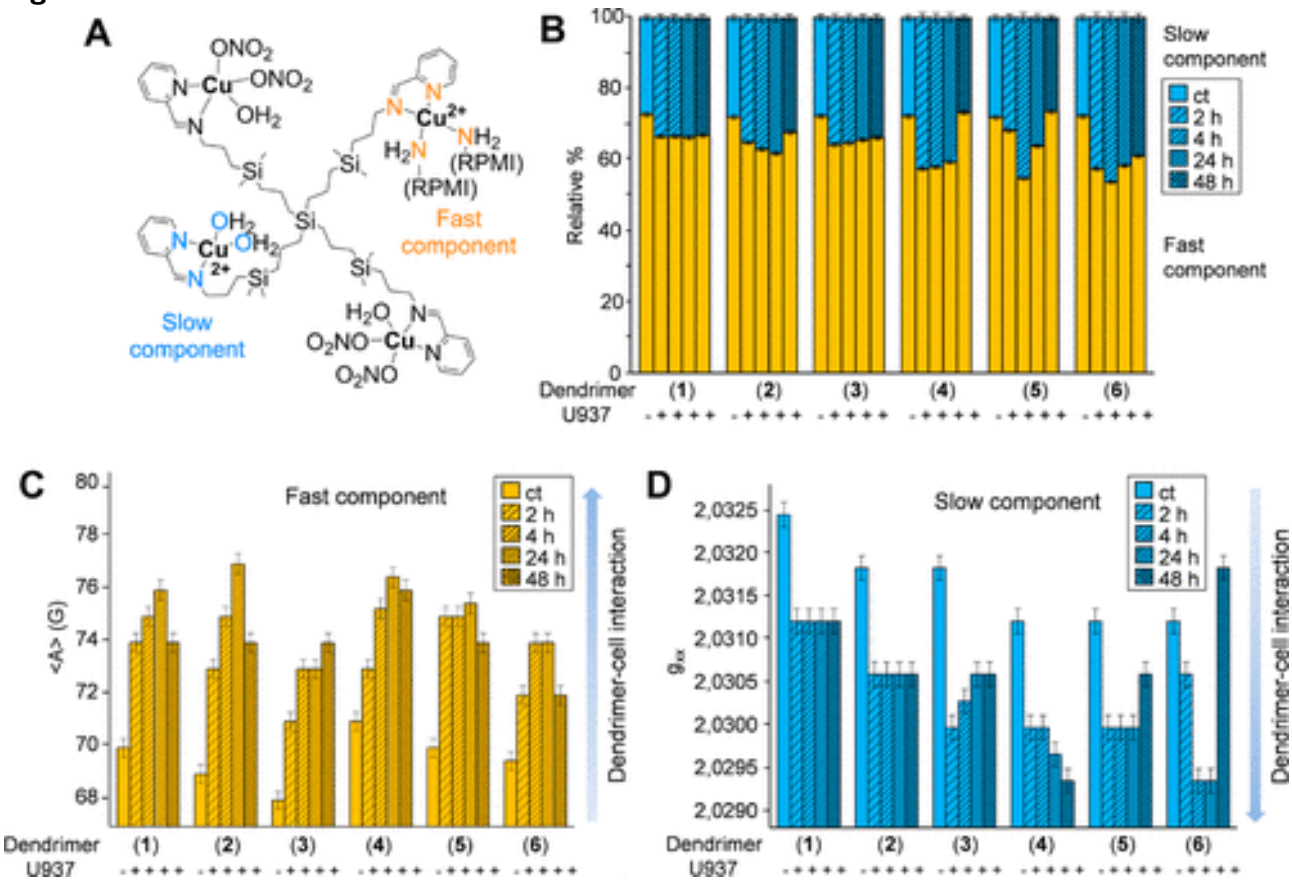

Figure 2. Analysis of the EPR spectra of metallodendrimers **1**–**6** in the absence (ct) and presence of U937 tumor cells at different time points (2–48 h). (A) Different Cu(II) environments, leading to the fast and slow components in EPR spectra, using G_1-$Cu(ONO_2)_2$ (**2**) in the RPMI medium as an example. (B) Relative percentages of the spectral components. (C) Comparison of ⟨A⟩ for the fast component. An increase in ⟨A⟩ indicates an increase in the dendrimer–cell interaction. (D) Comparison of g_{xx} for the slow component. A decrease in g_{xx} indicates an increase in the dendrimer–cell interaction.

The magnetic parameters from computation (the computed line, in red, is also shown in Figure S1) of the fast component of dendrimer **2** in RPMI, ⟨A⟩ ≥ 69 G and ⟨g⟩ ≥ 2.123, compared with literature ones, (12,22−25,27−33) indicate the formation of a square planar (orthorhombically distorted) Cu(II)-N_4 coordination. The nitrogen sites are the iminopyridine groups at the dendrimer surface, and nitrogen sites present in the RPMI medium are listed above. High

mobility is supported by a correlation time for motion τ = 42 ps. The slow component is visible in Figure S1 as a peak at a relatively low intensity and high magnetic field. The subtraction of the fast component allowed us to obtain the slow component and compute it. An example of the computation of this component is shown in Figure S2. For a better comparison, Table ST1, also included in the Supporting Information, lists the g_{ii} and A_{ii} main magnetic parameters for selected examples of fast and slow components. The significant increase of τ from the fast to the slow component indicates that the ions are trapped at the dendrimer interface. The values ⟨g⟩ = 2.15 and ⟨A⟩ = 58 G used for computation (red line in Figure S2) also indicate different coordinations of these trapped ions with two nitrogen and two oxygen ligand groups (Cu(II)-N_2O_2).

The addition of PBMC to the Cu(II) metallodendrimers produced negligible variations in the EPR spectra. Overall, EPR analysis indicated that PBMC barely interacted with the dendrimers, and these results are not henceforth discussed. Conversely, a different situation was observed when U937 tumor cells were added to the dendrimers. After 24 h of incubation with U937 cells, dendrimer G_1-Cu(ONO_2) (**2**) revealed a spectrum (Figure S1, bottom), where the fast component was computed using higher ⟨A⟩ (77 G) and τ (58 ps) values and a lower ⟨g⟩ value (2.119) with respect to the absence of these cells. Furthermore, the relative percentage of the slow component was higher in the presence (35%) than in the absence (27%) of U937 cells. Finally, the g_{xx} value of the slow component was lower in the presence (2.0305) than in the absence (2.0317) of U937 cells. Overall, these parameters indicate an interaction, mainly electrostatic through the Cu(II) complexes, between the dendrimer and the cancer cells.

The fast components for all dendrimers in the absence and in the presence of U937 cells at different incubation times (2, 4, 24, 48 h) were computed, and the calculated ⟨A⟩ values are shown in Figure 2.C. For all dendrimers, ⟨A⟩ increased by adding the U937 cells and by increasing the incubation time up to 24 h. This indicates a progressively positive interaction between the dendrimers and U937 cells over time. After 24 h, a decrease of ⟨A⟩ was observed, which may be provoked by cell degradation. The disruption at the membrane level well justifies a weakening of the Cu(II)-ligand binding strength and increased interaction with oxygen sites at the expense of the nitrogen sites. The results at the latest incubation time (72 h) were not reported because of poor reproducibility, but they were, in any case, in line with the trend shown from 24 to 48 h. The change of ⟨A⟩ over time was different among the evaluated dendrimers. In the absence of cells, chloride dendrimers showed slightly higher values than nitrate ones, indicating stronger interactions of the ions with the former than with the latter dendrimers. Furthermore, the strength of interaction decreases with each generation. This may be accounted for by a perturbative effect of neighboring Cu(II) complexes. Indeed, the ⟨A⟩ values for G_2dendrimers increased less than for the other generations at all incubation times. This means that the increased density of surface groups of G_2 dendrimers is perturbative for interactions at the dendrimer interface. Interestingly, G_1-Cu(ONO_2)$_2$ (**2**) showed the highest variation at 4 and 24 h, while G_1-$CuCl_2$ (**5**) showed a significant variation already at 2 h and then ⟨A⟩ barely changed until 24 h. This means that, for a fraction of complexes producing the fast component, **5** quickly interacted with the cells, while **2** required 24 h to produce stronger surface interactions with respect to the other dendrimers. Unexpectedly, G_0 dendrimers behaved quite oppositely: G_0-$CuCl_2$ (**4**) gave higher ⟨A⟩ values at 24–48 h, but G_0-Cu(ONO_2)$_2$ (**1**) interacted stronger at earlier times. The relatively strong and persistent interaction of G_0-$CuCl_2$ (**4**) is justified considering that this small, flexible, and quite hydrophobic molecule was particularly great at adhering at and then entering the cell membrane. G_2-Cu(ONO_2)$_2$ (**3**) showed interactions at 2–4 h; then, this effect decreased over time.

Further additional information was achieved from the analysis of the slow components. Its relative percentage changed for the different dendrimers from the absence to the presence of U937 cells as a function of the incubation time (Figure 2B). These variations were accompanied by a variation in the binding ability, proved by the variation of the position of the minimum of the peak at high field.

This variation reflected the variation of the g_{xx} parameter (Figure 2D), which therefore became the most reliable parameter in the computation of the slow component, together with its relative percentage, to describe the binding properties for the slow component. In detail, the following is true: the lower the g_{xx}, the stronger the interaction. Comparing the results for the fast and the slow components in Figure 2, different dendrimer–cell interactions were observed over time with an emphasis on the increase of % and decrease of g_{xx} when U937 cells were present. If cells were not present, the slow-component percentage remained invariant among the different dendrimers. However, the interaction strength measured by g_{xx} was stronger for the dendrimers with the chloride counterion than for nitrate-containing ones, and increased among the nitrate dendrimers, from G_0 to G_1 and G_2. These results confirm that $CuCl_2$ complexes are more stable than $Cu(ONO_2)_2$ complexes, and the interactions with the cells perturb the complex stability mainly for the chloride counterion. Surprisingly, G_1-$CuCl_2$ (**5**), which showed a quick interaction for the fast component, at 2 h revealed the lower percentage of the slow component among the various dendrimers, even if g_{xx} values indicated an increase in interaction strength since 2 h. The relatively low % at 2 h is probably related to a barrier effect played by the fast-moving but better-interacting complexes. However, at 4 h, the % of the slow component for **5** significantly increased but, at 24 h, decreased again to be the minimum at 48 h. Therefore, this dendrimer quickly interacted, but the slow and fast cell-binding conditions competed with each other. The slow conditions (strong interactions) only won at 4 h. A completely different behavior was found for G_2-$CuCl_2$ (**6**). This dendrimer showed low values of ⟨A⟩ for the fast component, while it showed the highest percentage of the slow component in the presence of the cells at all incubation times. This means that dendrimer **6** persistently interacted with the cell membrane, in agreement with the results on membrane models. (22) However, the interaction process was slower for dendrimer **6** than for dendrimer **5**, requiring more than 4 h to display a preferential interaction (lowest g_{xx} value). After 48 h, dendrimer **6** was still interacting, but cell degradation occurred, and the interaction strength significantly decreased (increase in g_{xx} values). The results from G_0-$CuCl_2$ (**4**) were also peculiar, since the interaction strength measured by g_{xx}increased progressively up to 48 h. At this time, complex **4** displayed the strongest interaction (lowest g_{xx}) but a small percentage of the interacting component. In conclusion, dendrimer **4**showed a strong and persistent interaction, as confirmed by the fast component results.

With regard to nitrate dendrimers, G_0-$Cu(ONO_2)_2$ (**1**) showed weaker interactions of the slow-moving ions than G_0-$CuCl_2$ (**4**), both in the absence and in the presence of U937 cells. These interactions remained invariant over the incubation time range. Therefore, G_0-$Cu(ONO_2)_2$ (**1**) interacted well with U937 cells at the external surface. This most likely provoked a harmful and prolonged internalization into the cells, probably via phagocytosis, with a consequent invariance in the perturbation of the slow-moving ions over time. G_1-$Cu(ONO_2)_2$ (**2**) displayed stronger interactions than **1**, also invariant over time, but a small increase in the percentage of the slow component was observed until 24 h. This increase corresponded to the relatively high increase in interactions at the external surface, which indicates that this dendrimer may be active in partially degrading the U937 cells. Conversely, for G_2-$Cu(ONO_2)_2$ (**3**), the percentage of the slow component changed poorly over time, while the interaction strength increased at 2 h and then progressively decreased. This held true for both the fast and the slow component,

indicating a perturbation played by neighboring Cu(II) complexes, probably due to the presence of a higher density of polar NO_3 groups. This probably stabilized the complex, leading to lower toxicity. In any case, the interactions were favored for G_2-$CuCl_2$ (**6**) with respect to G_2-$Cu(ONO_2)_2$ (**3**), due to the ability of **6** to enter the cell membrane, stabilize at the dendrimer–cell interface and potentially lead to eventual phagocytosis.

These results are in agreement with previous results that demonstrate a unique interaction of dendrimers toward cell membranes by using both model membranes and real cells. (11,12)Model membranes, such as liposomes and micelles, mimic the structural organization of cellular membranes and, making use of a range of characterization techniques, provide physical insights into the interactions between dendrimers and cell membranes. (34) In the present case, previous studies using CTAB micelles and lecithin liposomes have provided valuable insight into the interactions between Cu(II) carbosilane metallodendrimers and model membranes. (22) It was found that both the relative amount of interacting component and the strength of the interaction between dendrimers and model membranes increase for higher dendritic generations as well as for chloride-containing dendrimers, compared to nitrate ones. The results found on U937 cells were perfectly in line with the previous ones on the model membranes, showing that they are satisfactory models for the cancer cell membrane. However, interestingly, the former *in vitro* study also showed lower toxicity in cancer cells due to this stabilization effect. (22)

Further conclusions can be obtained studying the interactions of different types of dendrimers with the cells. The presence of cationic groups in a dendrimer promotes the binding to the negatively charged cell surface, but is also responsible for potential toxicity, thus requiring a good compromise between effective internalization and toxicity. For example, the interaction of cationic PAMAM dendrimers toward HeLa cells increased with the generation and, thus, the amount of positive charges. (14,15) Importantly, herein we demonstrated that close Cu(II) complexes at the surface of Cu(II) carbosilane metallodendrimers exerted a perturbative effect on complex stability with increasing generations. This translated into decreased interaction strength for G_2 dendrimers. The interaction is not only dependent on the amount of cationic groups but also on their distribution and interacting ability. The interactions and kinetics of dendrimer internalization are also modulated by the type of cells. G_4-PAMAM dendrimers underwent fast endocytosis in HepG2 cells; (35) a very slow internalization and a high membrane affinity in PC-12 cells; and a complete uptake in 4 h in HeLa, astrocytes and lung fibroblasts. (14) According to the EPR study, our metallodendrimers showed a maximum interaction with U937 cells membrane at 24 h, thus confirming a stronger interaction with the cell membranes and a slower internalization mechanism, while ruling out the interactions with PBMC according to the absence of spectral variations. Overall, it can be concluded that cationic carbosilane metallodendrimers cross cell membranes but with different dynamics depending on the type of dendrimer, membrane chemical composition, and cell-type recycling kinetics.

As previously mentioned, the dendrimer–cell uptake depends on different parameters such as generation, functionalization, concentration, and surface charge of dendrimers, as well as the cell type. Within cells, the dendrimer's fate depends on the mechanism of cellular uptake. As an example, endocytosis has been reported as the main cellular uptake mechanism of PAMAM dendrimers, but passive diffusion has also been reported. The cytotoxic response of PAMAM dendrimers depended on the cellular uptake pathway; in turn, this is influenced by dendrimer-membrane interactions. To gain further insight into the intracellular fate of Cu(II) carbosilane metallodendrimers, *in vitro* experiments were performed.

3.2. *In Vitro* Evaluation of PBMC and U937 Myeloid Cell Line Response to Metallodendrimers Administration

In order to translate the results obtained through EPR studies to a more strictly biological analysis, subsequent *in vitro* experiments were performed, which evaluated the cytostatic and cytotoxic behavior of the compounds in the tumor cell line U937, as well as in healthy peripheral blood lymphocytes (PBMC) from donors. Lower dendrimer concentrations (10^{-5} M) were used for the biological assays, in comparison to those used in the EPR analysis (10^{-3} M), aiming for a compromise between viability and biological effect (Figure S2). Additional sublethal effects regarding mitochondria function, lysosomal compartment, and autophagic organelle involvement were studied and are herein presented.

3.2.1. Cytotoxic and Cytostatic Behavior

Cytotoxicity and cytostasis are desirable properties for antitumor drugs. Cytotoxic agents produce cell death and eventual tumor shrinkage, whereas cytostatic agents inhibit tumor growth through the alteration of their metabolism and blockage of cell division but without direct toxicity. (36) The cytostatic and cytotoxic properties of metallodendrimers **1**–**6** were evaluated through flow cytometry after 24, 48, and 72 h cell treatment. The results are shown in Figure 3, including absolute cell count (A, B) and dead cell count (C, D) by staining with fluorescent probe Propidium Iodide (PI). The experiments depict a different scenario for PBMC and U937 cells: in U937, a cytostatic and cytotoxic behavior was observed already at 24 h, whereas, in PBMCs, a significant cytotoxic input occurs only at 72 h. These results match the conclusions from EPR analysis.

Figure 3

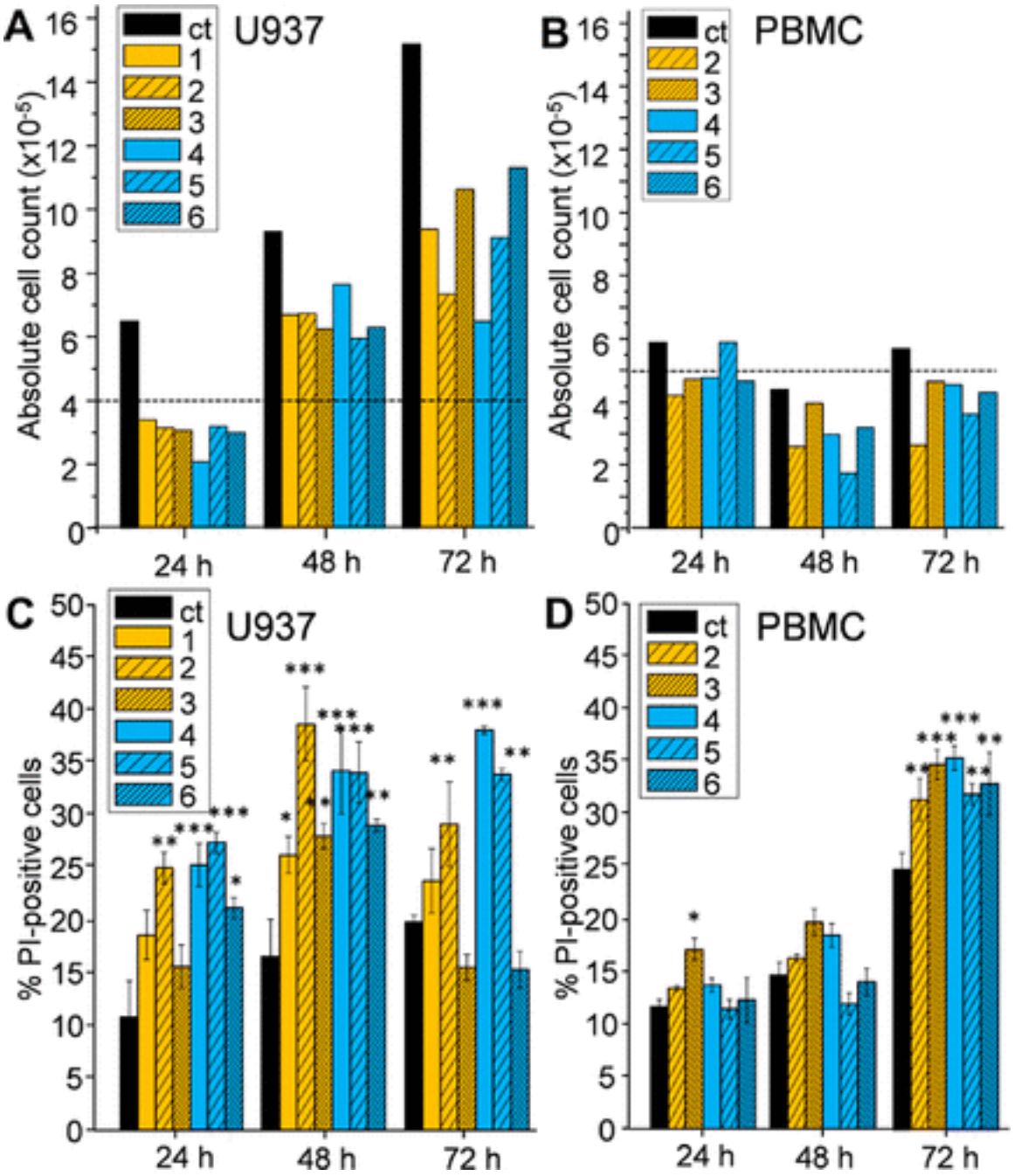

Figure 3. Evaluation of metallodendrimers toxicity on the tumor cell line U937 ((A) absolute cell count; (C) % of PI-positive cells) and on healthy lymphocytes ((B) absolute cell count; (D) % PI-positive cells). The dashed line indicates the absolute cell count at t = 0.

Both metallodendrimer families are antiproliferative (cytostatic) and moderate cytotoxic agents for U937 tumor cells (Figure 3A,C). Control cells appear in exponential cell growth, unlike dendrimer-treated cells, confirming the cytostatic properties of these dendrimers. Supravital PI uptake measures the cytotoxicity of the compounds. Already after 24 h treatment, significant cell death is observed for first-generation dendrimers **2** and **5**, as well as for the G_0 complex **4**due to a mainly cytotoxic effect. These results are supported by EPR analysis, which suggests a probable harmful effect of compounds **2** and **5** against U937 cells, but the stabilization of the chloride complex **5** at the external cell surface seems to delay the internalization of the dendrimer into the cells. Also, the cytotoxicity of **4** is supported by the EPR results since this small, flexible, and quite hydrophobic compound easily penetrates the cell membrane inducing a certain degree of cell death. Second-generation

compounds **3** and **6** exhibit a similar mild effect on both viability and proliferation. EPR results also show that the interacting ability between the complexes and U937 cells decreases from G_0 to G_2, probably due to an increase in the density of surface groups that provokes perturbation between adjacent Cu(II) complexes.

The Cu(II) metallodendrimers barely affected the PBMC (Figure 3B,D). The absolute cell number was only visibly reduced after 48 h treatment with first-generation dendrimers **2** and **5**, ascribed to a direct cytotoxic effect (the cytostatic effect is ruled out, due to the nonproliferating feature of normal lymphocytes). Nitrate metallodendrimer **2** showed a faster mechanism, probably necrosis and/or necroptosis, than the chloride counterpart **5** and the second-generation analogue **3**. Unfortunately, no reproducible results were obtained for complex **1**. The number of **2**-treated lymphocytes directly decreases, before the individuation of PI positivity, while **3**-treated cells suffer a lower decrease, although revealing a relevant and significant number of PI-positive events. It was possible to distinguish early apoptotic and necrotic cells through the different PI fluorescent intensity (Figure S2). This effect is especially remarkable for the nitrate-dendrimer **2**, with a significantly higher activity than the mononuclear and second-generation counterparts **1** and **3**. Again, the higher toxicity of dendrimer **2** was predicted by the EPR analysis. Such differences among the different generation analogues are diluted in the chloride-containing family.

Anticancer therapy usually induces apoptotic (37) and/or autophagic cell death, (38) direct necrotic cell death (39) or senescence. (40,41) While cancer cells are highly proliferative, most normal somatic cells (as PBMCs) present a nonproliferative, postmitotic state, whose features partially explain the specificity observed toward tumor cells because the activity of several cytotoxic agents is dependent on cell-cycle progression. (42)

Cu(II) carbosilane dendrimers are more cytotoxic toward U937 tumor cells than other cationic dendrimers. For example, treatment with second-generation dendrimer **6** at 10^{-5} M, bearing 8 iminopyridine Cu(II) complexes, produced a 10% increased death compared to nontreated cells. A concentration 40 times higher of a G_2-polypropyleneimine dendrimer, comprising 8 $-NH_2$peripheral groups, is necessary to reach a comparable cytotoxic response in U937 cells. (43)Unlike PPI and PAMAM dendrimers, which showed U937 toxicity in a time- and generation-dependent way, (43) our Cu(II) metallodendrimers follow the pattern previously observed with carbosilane analogues: (23) First-generation complexes **2** and **5** are the most effective among the different generation complexes.

Aiming for a deeper understanding of the mechanisms responsible for U937 cell death, we focused on analyzing the sublethal effects on the residual cells from the previous experiments. The effect of the metallodendrimers on the mitochondria function, the lysosomal compartment, and the involvement of autophagy was analyzed. The results, which are shown below, indicate that the pathways involved in death processes include the autophagic vacuole formation and the mitochondria–lysosome axis.

3.2.2. Effect on Mitochondria Transmembrane Potential

The mitochondrial transmembrane potential ($\Delta\Psi_m$) drives the production of ATP in the cell. (44)At high $\Delta\Psi_m$, the mitochondrial respiratory chain generates ROS in an exponential ratio to $\Delta\Psi_m$, being potentially harmful to mitochondria and ultimately to the cell. On the other hand, sustained low values of $\Delta\Psi_m$ lead to insufficient ability to produce ATP as well as “reductive stress”, which is as detrimental to homeostasis as oxidative stress. Normal cell functioning requires stable levels of intracellular ATP and $\Delta\Psi_m$, and a continued alteration of these factors may compromise the viability of the cells. In some diseases such as cancer, the mitochondria exhibit significantly higher $\Delta\Psi_m$, compared to normal cells, and can be used as a therapeutic antitumor target. (45) The changes in $\Delta\Psi_m$ after treatment with compounds **1**–**6** were evaluated

through tetramethylrhodamine ethyl ester (TMRE) labeling, and the results are shown in Figure 4.

Figure 4

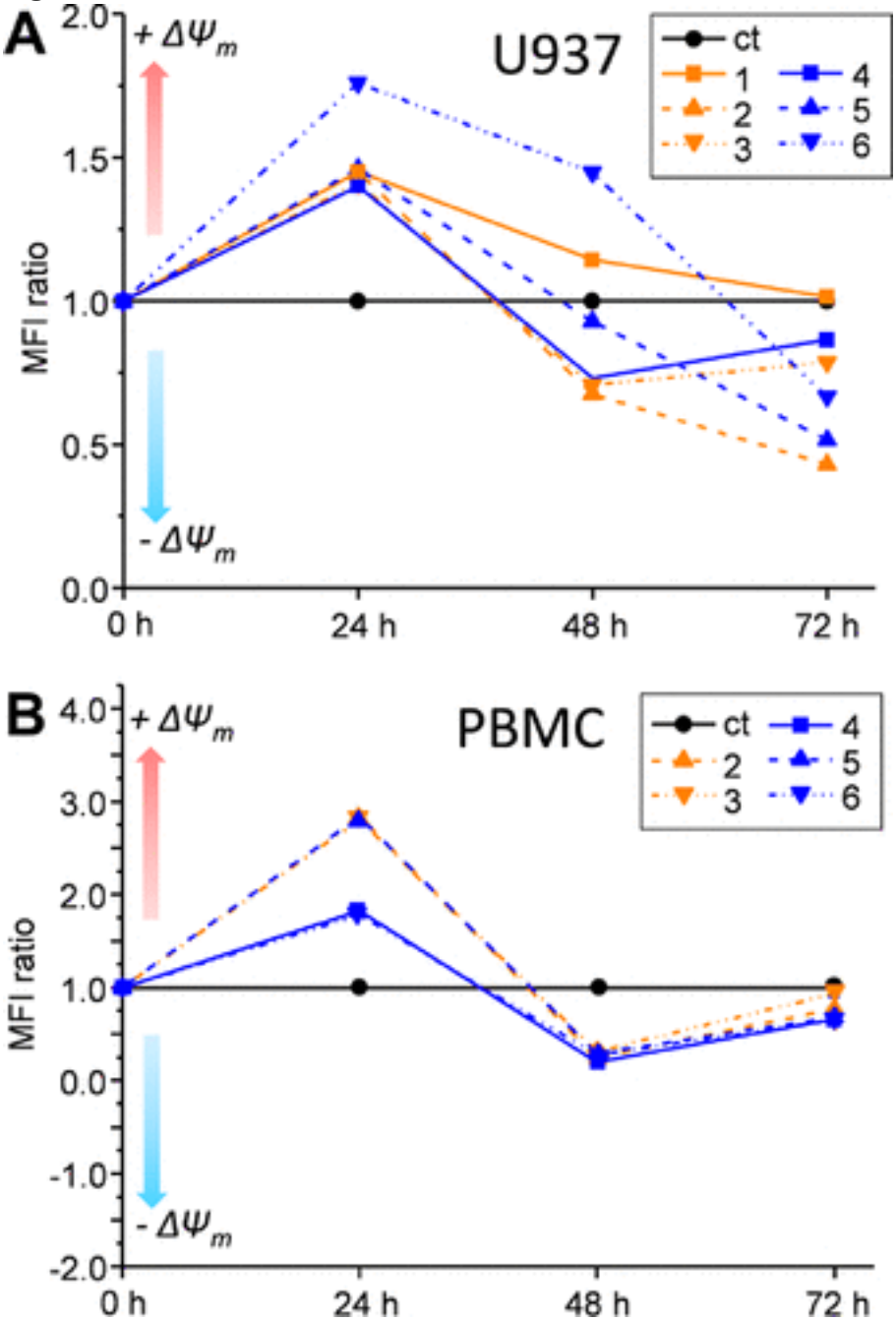

Figure 4. Changes in the mitochondria membrane potential ($\Delta\Psi_m$) in U937 cells (A) and PBMC (B) after treatment with metallodendrimers **1**–**6** measured through TMRE labeling. The error bars have been deleted to facilitate the reading but can be found in Figure S4.

The treatment of U937 cells with Cu(II) complexes **1**–**6** (Figure 4A) produced an initial pro-oxidative effect, revealed by an increase in TMRE fluorescence at 24 h, especially remarkable for second-generation metallodendrimer **6**. This result was expected on the basis of the peculiar interaction behavior shown by the EPR analysis of this dendrimer. However, such a strong and persistent interaction increases the mitochondria transmembrane potential but decreases the toxicity. As previously reported, mitochondrial membrane hyperpolarization may be related to a significant production of reactive oxygen species (ROS). (46,47) This production of ROS is exponentially dependent on $\Delta\Psi_m$ and potentially harmful to the cell and detrimental

to homeostasis. Furthermore, this initial hyperpolarization produced by Cu(II) metallodendrimers matches the one observed for nanosized copper particles. (48) At 48 h, the membrane potential collapsed, particularly for metallodendrimers **2**, **3**, and **4**, and kept decreasing at 72 h for first-generation dendrimers **2** and **5**. Together with complex **6**, also complex **1** exhibited a prolonged pro-oxidative effect until 48 h, in agreement with the EPR results showing a quick interaction with the cell surface, which persists over time. These findings are in agreement with the data on viability and proliferation in Figure 3: **2**-treated U937 cells did not show any relevant partial recovery at 72 h, whereas compound **1** continues to increase the membrane potential, suggesting a delayed but prolonged effect. Also, this finding is supported by EPR results, since **1**showed an invariance in the perturbation of the slow-moving Cu(II) ions over time.

A different situation is observed in PBMC. The metallodendrimers produced a stronger pro-oxidative effect at 24 h, if compared to U937, followed by a significant decrease at 48 h for all compounds, which is mildly recovered after 72 h. Recent findings demonstrated that tumorigenesis requires functional mitochondria; accordingly, the mitochondrial electron transport chain (ETC) emerges as a potential target in antitumor treatment. (49) Although ETC complexes were not directly evaluated here, it is known that ETC and ATP production are strictly correlated. (50) As most somatic cells are in a nonproliferative state, the features associated with the ETC and their mitochondria membrane potential in quiescence could account for some of the specificity observed toward tumor cells.

Copper is an essential element with two fundamental intracellular functions, related to its redox ability as a cofactor of either mitochondrial cytochrome c oxidase or the Cu/Zn superoxide dismutase, involved in detoxifying ROS. It has been reported that a surplus of copper within mitochondria can initiate oxidative damage and induce the destruction of this organelle. (51) In our case, the Cu(II) atoms are chelated through the iminopyridine ligands, leading to stable complexes which hinder the release of metal ions. However, it is well-known that the nitrate ligands in Cu(II) metallodendrimers **1**–**3** are more labile than the chloride ligands in compounds **4**–**6** and can be easily released in water solutions. The EPR results are in line with this finding. Accordingly, the higher overall positive charge in the nitrate systems could explain their different effect on the mitochondria membrane potential. For example, first-generation nitrate complex **2**is more effective in decreasing $\Delta\Psi_m$ in U937 cells at 48 and 72 h than its chloride counterpart **5**.

Interestingly, the nature of the metal complex located at the periphery of the dendritic scaffold dictates the effect on the mitochondria membrane potential. Alternative metallodendrimers comprising the same carbosilane dendritic scaffold herein used and decorated with ruthenium(II) complexes have been evaluated for their antitumor activity toward acute promyelocytic leukemia HL60 cells. (52)

The study revealed a general mitochondrial hyperpolarization, where $\Delta\Psi_m$ increased when increasing metallodendrimer concentration (from 0.5 to 5.0 μM) and generation (from G_1 to G_2). A time-dependence was also observed, finding the maximum hyperpolarization at 3 h for G_1 and 72 h for G_2. The Cu(II) metallodendrimers, however, exhibited the highest hyperpolarization at 24 h and then a progressive decrease in $\Delta\Psi_m$, reaching values below the potential of nontreated cells.

3.2.3. Effect on Lysosome and Autophagosome Routes

After the uptake of nanomaterials by either phagocytic or nonphagocytic mechanisms, internalization into lysosomes is a frequent event. These organelles represent an extremely hostile environment due to their low pH and the variety of hydrolytic enzymes that can degrade most nanomaterials, except the most biopersistent. We evaluated the involvement of

lysosomes after 24 h of dendrimer administration to U937 using LysoTracker. The results indicated that the lysosome pathway was involved after 24 h treatment of the copper metallodendrimers with U937, especially for compounds **1** and **6**, the latter displaying a significant peak in lysosome number/acidity (Figure 5A).

Figure 5

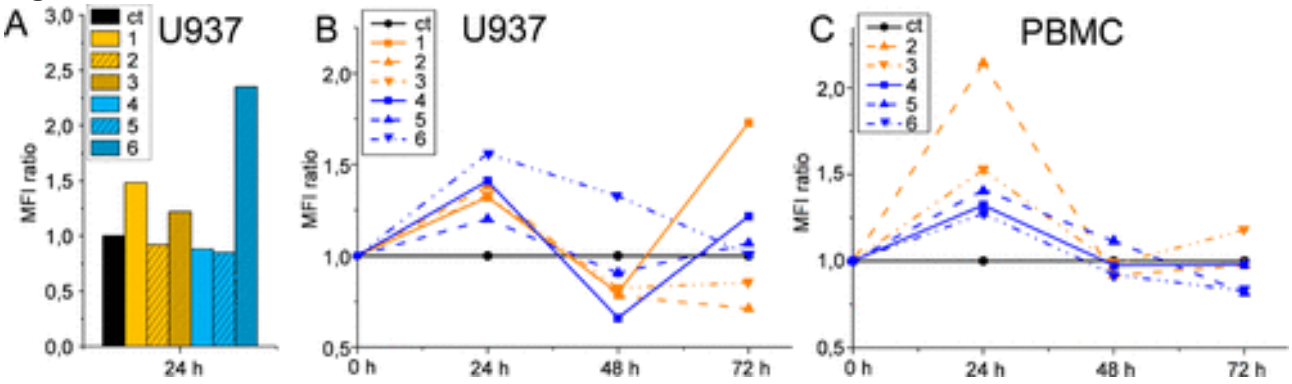

Figure 5. (A) Involvement of the lysosome pathway in U937 cells after treatment with compounds **1**–**6**, measured using LysoTracker green. (B, C) Autophagy perturbation induced by treatment with the different compounds and measured using MDC labeling in U937 and PBMC. The error bars have been deleted to facilitate the reading but can be found in Figure S5.

In addition to the endolysosomal pathway, nanomaterials can also induce autophagy. (53)Autophagy is a catabolic strategy to degrade cellular components through lysosomes and thus mitigate cellular stress. In cancer therapy, it can act as a cytoprotective or cytotoxic mechanism in a context-dependent fashion, (54) fostering a controlled cell death or supporting the survival of cancer cells by providing metabolic precursors. Furthermore, it plays many different roles in lymphocyte development and function. (55) It has been found that PAMAM dendrimers (G_5-NH_2) induce both reactive oxygen species and autophagy flux in neuronal cells. (56)

To elucidate lysosome–autophagosome routes after treatment with the Cu(II) metallodendrimers, we performed a monodansylcadaverine (MDC) labeling assay, a specific marker of autophagic induced vacuoles (AIVs) (Figure 5B,C). The increase in mean fluorescence intensity (MFI) indicates an alteration of autophagy flux, with the accumulation of autophagosomes, whereas the decrease represents an effective loss or disruption of the same organelles. In U937, cell treatment with nitrate complexes **1**–**3** produced a mild increase at 24 h and a mild decrease at 48 h, with no clear dependence on dendrimer generation. The only remarkable increase was observed for monometallic complex **1** after 72 h, which correlates to a reduction of PI positivity and with the still impaired proliferation. In addition to the cytoprotective form of autophagy, a cytostatic form of autophagy can be induced, as recently reported. (57)

Chloride dendrimers **4**–**6** showed certain heterogeneity, especially second-generation dendrimer **6**. At 24 h, dendrimer **6** displayed the highest MFI value for MDC labeling, in agreement with data from LysoTracker green assay, and constantly decreased to MFI = 1 at 72 h. In this case, too, the peculiar stability and interactions with the cell membrane for dendrimer **6**, as tested by EPR, support the occurrence of a phagocytosis process with the involvement of lysosomes.

Conversely, compounds **4** and **5** exhibited a decrease at 48 h and an increase at 72 h, quite remarkable for monometallic complex **4**. We already discussed the ability of dendrimer **4** to penetrate the cell membrane, producing cell death. Overall, we can conclude that compounds **1**and **6** are the most efficient in autophagosome induction, followed by compound **4**. Regarding PBMC (Figure 5C), autophagy seems more upregulated in nitrate-

treated cells, compared to the chloride counterparts. In particular, first-generation metallodendrimer **2** induces an important formation of autophagic vacuoles after 24 h of treatment, probably as a cytoprotective mechanism according to the absence of toxicity observed in Figure 3D.

Altogether, these results suggest that treatment with carbosilane copper metallodendrimers induce death processes through the mitochondria–lysosome axis as well as autophagic vacuole formation. The dendrimers seem to stabilize different subcellular compartments, playing an important role in the exerted toxicity. They may cause lysosomal overload with indigestible material, including copper, disrupting the fusion of lysosomes with other cell compartments and resulting in vacuole accumulation, as observed in our assays. Other cationic dendrimers, such as PAMAM dendrimers, induce the loss of mitochondrial membrane potential and lysosome membrane permeabilization, through a proton sponge mechanism. (58) Lysosome membrane permeabilization is a well-known cell death mechanism, which may result in mitochondrial outer membrane permeabilization or be contemporaneous, giving the subsequent induction of reactive oxygen species (ROS) generation and apoptosis, or even necrosis.

Nanomaterial-induced autophagy perturbation, both induction and blockade, has been widely reported, (59) with several plausible mechanisms including oxidative stress, mitochondrial damage, alteration of signaling pathways, or a simple attempt to degrade a foreign entity. The dysfunction of autophagy and lysosomal pathways is a potential cytotoxicity mechanism but may also be a potential therapeutic mechanism.

4. Conclusions

In search of efficient and selective antitumor therapies, copper(II) carbosilane dendrimers stand out due to their high stability, exceptional structure-to-property relationship, and unique interaction with cell membranes, which can be fine-tuned, altering the dendrimer generation and the metal counterion. This extraordinary interaction, which further explains the potent and selective cytotoxic behavior, has been studied through EPR in model cell membranes and herein confirmed in myeloid cancer (U937) and healthy (PBMC) cells.

EPR spectral computation showed that the Cu(II)-N_2O_2 coordination observed when the ions are trapped in slow motion at the dendrimer interface was perturbed or stabilized during the electrostatic interaction with the membranes of U937 cancer cells.

Importantly, these interactions were preferential with the cancer cells and weak or absent with healthy PBMCs. The interaction between the Cu(II) complexes and U937 cells progressively increased over the incubation time. Cell degradation started probably after dendrimer uptake, when the disruption at the membrane level well justifies the weakening of the Cu(II)-ligand binding strength measured by EPR, and increased interaction of Cu(II) with oxygen sites at the expenses of nitrogen sites. The biological *in vitro* assays confirmed that Cu(II) metallodendrimers are cytostatic and moderate cytotoxic agents for U937 tumor cells, while barely affecting healthy PBMCs, in part explained by the nonproliferating nature of PBMCs. They altered the mitochondria transmembrane potential of U937 cancer cells, producing an initial pro-oxidative effect at 24 h and a subsequent collapse of up to 72 h. These metallodrugs perturbed the lysosome pathway and the autophagy flux in U937 cells, increasing the formation of autophagic vacuoles at 24 h, which were progressively disrupted over time. A similar effect was observed in PBMC, but the initial pro-oxidative effect is buffered over time, recovering the control values at 72 h. The increased formation of autophagic vacuoles at 24 h and subsequent degradation may be related to a cytoprotective response, considering the absence of toxicity

at 24 and 48 h. This effect is particularly remarkable for G_1-$Cu(ONO_2)_2$ (**2**), with an extremely high increase in autophagy after 24 h of treatment.
The structural perfection of Cu(II) metallodendrimers provided valuable insight into the influence of dendritic generation and the metal counterion on the interaction with cancer cells and the subsequent therapeutic effect. Overall, the following conclusions can be drawn:

1. Both in the absence and in the presence of cells, the strength of interactions of the ions was stronger (more stable Cu(II) complexes) with chloride dendrimers than with the nitrate ones and may lead to a different uptake mechanism. For example, G_0-$CuCl_2$ (**4**) gives a strong and persistent interaction with U937 cells after 24 h, as this small, flexible, and hydrophobic complex easily penetrates the cell membrane and leads to cell death. However, G_0-$Cu(ONO_2)_2$ (**1**) interacts stronger at the external surface and at shorter times, producing a harmful and prolonged internalization of **1**through phagocytosis, with a consequent invariance in the perturbation of the slow-moving ions over time.

2. The interaction strength decreased with the increase in generation, probably due to the increase of surface-group density that provokes perturbation between adjacent Cu(II) complexes. Nevertheless, this does not exclude strong and persistent interactions with the cell membrane with second-generation metallodendrimers such as G_2-$CuCl_2$ (**6**), in agreement with the results on membrane models, (22) favoring phagocytosis and a persistent mitochondria hyperpolarization.

3. A strong and persistent interaction with the cell membrane, such as that observed for metallodendrimers **1** and **6**, favors phagocytosis, increases the mitochondria transmembrane potential, and leads to a prolonged formation of autophagy vacuoles that degrade cellular components, as cytostatic-related autophagy. Importantly, such persistent interactions decreased metallodendrimer toxicity.

4. The structural features of first-generation metallodendrimers G_1-$Cu(ONO_2)_2$ (**2**) and G_1-$CuCl_2$ (**5**), such as the metal complexes distribution and the hydrophilic–hydrophobic balance, induced a remarkable cytotoxicity in U937 cells already at 24 h, coinciding with an initial pro-oxidative effect, and an outstanding collapse of mitochondria transmembrane potential up to 72 h, in agreement with their higher toxicity. A simple exchange of counterion modified the interaction speed: G_1-$CuCl_2$(**5**) interacted quickly (2–4 h), but the interactions were not persistent, as shown by the EPR results; the biological data on **5** showed that the labile interactions at the external surface delayed the internalization in the cells. Conversely, G_1-$Cu(ONO_2)_2$ (**2**) required 24 h to produce strong and persistent interactions at the U937 cell surface (EPR results). These interactions favored, for **2**, a higher activity and faster cytotoxic mechanism (mainly at 24–48 h), probably necrosis and/or necroptosis, than the chloride counterpart **5**. The fast and selective cytotoxic response of metallodendrimer **2** in myeloid cancer cells well justifies its selection as the

most promising candidate for further anticancer evaluation, consistent with our previous study toward resistant prostate cancer. (22) Complex **2** reduced the proliferation of PC3 cells, their adhesion to collagen type-I, and the tumor size up to 37% in an *ex vivo*mice model.

The potency and selectivity of Cu(II) metallodendrimers in myeloid cancer cells open new avenues in the use of nanosized metallodrugs for the treatment of leukemia, which cannot benefit from the well-known enhanced permeation and retention effect that improves the anticancer effect of nanodrugs in solid tumors.

SUPPORTING INFORMATION

The Supporting Information is available free of charge at Examples of EPR spectra and computations for selected samples, examples of cytometric contour plots to illustrate PI positivity, changes in mitochondria membrane potential, and formation of autophagic-involved vacuoles

AUTHOR INFORMATION

Barbara Canonico – orcid.org/0000-0003-338371SX
Riccardo Carloni − orcid.org/0000-0001-8052-2013X
Natalia Sanz del Olmo – orcid.org/0000-0001-9946-8073
Stefano Papa – orcid.org/0000-0001-9291-0527
Maria Gemma Nasoni − orcid.org/0000-0002-2078-7774
Alberto Fattori – orcid.org/0000-0001-6468-9140
Michela Cangiotti – orcid.org/0000-0002-5713-7740
F. Javier de la Mata – orcid.org/0000-0003-0418-3935
Maria Francesca Ottaviani − orcid.org/0000-0002-4681-4718
Sandra García-Gallego – orcid.org/0000-0001-6112-0450

CONFLICTS OF INTEREST

“There are no conflicts to declare”.

ACKNOWLEDGEMENTS

This research was funded by grants from CTQ2017-86224-P (MINECO), consortiums IMMUNOTHERCAN-CM B2017/BMD-3733, Project SBPLY/17/180501/000358 Junta de Comunidades de Castilla-la Mancha (JCCM) and the Comunidad de Madrid Research Talent Attraction Program 2017-T2/IND-5243. CIBER-BBN is an initiative funded by the VI National R&D&I Plan 2008–2011, Iniciativa Ingenio 2010, Consolider Program, CIBER Actions and financed by the Instituto de Salud Carlos III with assistance from the European Regional Development Fund. N.S.O. wishes to thank JCCM for a predoctoral fellowship. The authors thank DiSPeA and DiSB at the University of Urbino for the financial support for the EPR experiments and the cytometric experiments, and the Italian Ministry of University and Research for the financial support through PRIN 2017 project "FIBRES: a multidisciplinary mineralogical, crystal-chemical and biological project to amend the paradigm of toxicity and cancerogenicity of mineral fibres." This article is based upon work from COST Action CA17140 “Cancer Nanomedicine from the Bench to the Bedside” supported by COST (European Cooperation in Science and Technology). This work has been supported partially by a EUROPARTNER: Strengthening and spreading international partnership activities of the Faculty

of Biology and Environmental Protection for interdisciplinary research and innovation of the University of Lodz Programme: NAWA International Academic Partnership Programme.

NOTES AND REFERENCES

(1) Bray, F.; Ferlay, J.; Soerjomataram, I.; Siegel, R. L.; Torre, L. A.; Jemal, A. Global cancer statistics 2018: GLOBOCAN estimates of incidence and mortality worldwide for 36 cancers in 185 countries. Ca- Cancer J. Clin. 2018, 68 (6), 394−424.
(2) Wild, C. P., Weiderpass, E., Stewart, B. W., Eds.; World Cancer Report: Cancer research for cancer prevention; Lyon, France, 2019.
(3) Misra, R.; Acharya, S.; Sahoo, S. K. Cancer nanotechnology: application of nanotechnology in cancer therapy. Drug Discovery Today 2010, 15 (19), 842−850.
(4) Chaturvedi, V. K.; Singh, A.; Singh, V. K.; Singh, M. P. Cancer Nanotechnology: A New Revolution for Cancer Diagnosis and Therapy. Curr. Drug Metab. 2019, 20 (6), 416−429.
(5) Shang, L.; Nienhaus, K.; Nienhaus, G. U. Engineered nano-particles interacting with cells: size matters. J. Nanobiotechnol. 2014, 12,5.
(6) Dendrimers in biomedical applications; Royal Society of Chemistry: 2013; pp P001−204.
(7) Majoros, I. J.; Williams, C. R.; Baker, J. R., Jr. Current dendrimer applications in cancer diagnosis and therapy. Curr. Top. Med. Chem. 2008, 8 (14), 1165−79.
(8) Sharma, A. K.; Gothwal, A.; Kesharwani, P.; Alsaab, H.; Iyer, A. K.;Gupta, U. Dendrimer nanoarchitectures for cancer diagnosis and anticancer drug delivery. Drug Discovery Today 2017, 22 (2), 314−326.
(9) Ma, Y.; Mou, Q.; Wang, D.; Zhu, X.; Yan, D. Dendritic Polymers for Theranostics. Theranostics 2016, 6 (7), 930−47.
(10) Sk, U. H.; Kojima, C. Dendrimers for theranostic applications. Biomol. Concepts 2015, 6 (3), 205−17.
(11) Andreozzi, E.; Antonelli, A.; Cangiotti, M.; Canonico, B.; Sfara, C.; Pianetti, A.; Bruscolini, F.; Sahre, K.; Appelhans, D.; Papa, S.; Ottaviani, M. F. Interactions of Nitroxide-Conjugated and Non-Conjugated Glycodendrimers with Normal and Cancer Cells and Biocompatibility Studies. Bioconjugate Chem. 2017, 28 (2), 524−538.
(12) Ottaviani, M. F.; El Brahmi, N.; Cangiotti, M.; Coppola, C.; Buccella, F.; Cresteil, T.; Mignani, S.; Caminade, A. M.; Costes, J. P.; Majoral, J. P. Comparative EPR studies of Cu(II)-conjugated phosphorous-dendrimers in the absence and presence of normal and cancer cells. RSC Adv. 2014, 4 (69), 36573−36583.
(13) Kaur, A.; Jain, K.; Mehra, N. K.; Jain, N. K. Dendrimer Internalization: A Systematic Review. J. Colloid Sci. Biotechnol. 2015, 4 (2), 99−109.
(14) Albertazzi, L.; Serresi, M.; Albanese, A.; Beltram, F. Dendrimer Internalization and Intracellular Trafficking in Living Cells. Mol. Pharmaceutics 2010, 7 (3), 680−688.
(15) Albertazzi, L.; Fernandez-Villamarin, M.; Riguera, R.; Fernandez- Megia, E. Peripheral Functionalization of Dendrimers Regulates Internalization and Intracellular Trafficking in Living Cells. Bioconjugate Chem. 2012, 23 (5), 1059−1068.
(16) Mukherjee, S. P.; Lyng, F. M.; Garcia, A.; Davoren, M.; Byrne, H. J. Mechanistic studies of in vitro cytotoxicity of poly(amidoamine) dendrimers in mammalian cells. Toxicol. Appl. Pharmacol. 2010, 248 (3), 259−68.
(17) Zeng, X.; Zhang, Y.; Nyström, A. M. Endocytic Uptake and Intracellular Trafficking of Bis-MPA-Based Hyperbranched Copolymer Micelles in Breast Cancer Cells. Biomacromolecules 2012, 13 (11), 3814−3822.

(18) Kuo, J. H.; Jan, M. S.; Lin, Y. L. Interactions between U-937 human macrophages and poly(propyleneimine) dendrimers. J. Controlled Release 2007, 120 (1–2), 51–9.
(19) Lee, J. H.; Cha, K. E.; Kim, M. S.; Hong, H. W.; Chung, D. J.; Ryu, G.; Myung, H. Nanosized polyamidoamine (PAMAM) dendrimer-induced apoptosis mediated by mitochondrial dysfunction. Toxicol. Lett. 2009, 190 (2), 202–7.
(20) Lazniewska, J.; Milowska, K.; Zablocka, M.; Mignani, S.; Caminade, A.-M.; Majoral, J.-P.; Bryszewska, M.; Gabryelak, T. Mechanism of Cationic Phosphorus Dendrimer Toxicity against Murine Neural Cell Lines. Mol. Pharmaceutics 2013, 10 (9), 3484–3496.
(21) Wrobel, D.; Kolanowska, K.; Gajek, A.; Gomez-Ramirez, R.; de la Mata, J.; Pedziwiatr-Werbicka, E.; Klajnert, B.; Waczulikova, I.; Bryszewska, M. Interaction of cationic carbosilane dendrimers and their complexes with siRNA with erythrocytes and red blood cell ghosts. Biochim. Biophys. Acta, Biomembr. 2014, 1838 (3), 882–889.
(22) Sanz del Olmo, N.; Carloni, R.; Bajo, A. M.; Ortega, P.; Fattori, A.; Gómez, R.; Ottaviani, M. F.; García-Gallego, S.; Cangiotti, M.; de la Mata, F. J. Insight into the antitumor activity of carbosilane Cu(II)– metallodendrimers through their interaction with biological membrane models. Nanoscale 2019, 11 (28), 13330–13342.
(23) Sanz del Olmo, N.; Maroto-Díaz, M.; Gómez, R.; Ortega, P.; Cangiotti, M.; Ottaviani, M. F.; de la Mata, F. J. Carbosilane metallodendrimers based on copper (II) complexes: Synthesis, EPR characterization and anticancer activity. J. Inorg. Biochem. 2017, 177, 211–218.
(24) Rossi, J.-C.; Maret, B.; Vidot, K.; Francoia, J.-P.; Cangiotti, M.; Lucchi, S.; Coppola, C.; Ottaviani, M. F. Multi-Technique Characterization of Poly-L-lysine Dendrigrafts–Cu(II) Complexes for Biocatalysis. Macromol. Biosci. 2015, 15 (2), 275–290.
(25) Ottaviani, M. F.; Cangiotti, M.; Fattori, A.; Coppola, C.; Lucchi, S.; Ficker, M.; Petersen, J. F.; Christensen, J. B. Copper(II) Complexes with 4-Carbomethoxypyrrolidone Functionalized PAMAM-Dendrimers: An EPR Study. J. Phys. Chem. B 2013, 117 (45), 14163–14172.
(26) Budil, D. E.; Lee, S.; Saxena, S.; Freed, J. H. Nonlinear-Least-Squares Analysis of Slow-Motion EPR Spectra in One and Two Dimensions Using a Modified Levenberg–Marquardt Algorithm. J. Magn. Reson., Ser. A 1996, 120 (2), 155–189.
(27) Ottaviani, M. F.; Bossmann, S.; Turro, N. J.; Tomalia, D. A. Characterization of starburst dendrimers by the EPR technique. 1. Copper complexes in water solution. J. Am. Chem. Soc. 1994, 116 (2), 661–671.
(28) Ottaviani, M. F.; Montalti, F.; Turro, N. J.; Tomalia, D. A. Characterization of Starburst Dendrimers by the EPR Technique. Copper(II) Ions Binding Full-Generation Dendrimers. J. Phys. Chem. B 1997, 101 (2), 158–166.
(29) Ottaviani, M. F.; Valluzzi, R.; Balogh, L. Internal Structure of Silver–Poly(amidoamine) Dendrimer Complexes and Nanocomposites. Macromolecules 2002, 35 (13), 5105–5115.
(30) Appelhans, D.; Oertel, U.; Mazzeo, R.; Komber, H.; Hoffmann, J.; Weidner, S.; Brutschy, B.; Voit, B.; Francesca Ottaviani, M. Dense-shell glycodendrimers: UV/Vis and electron paramagnetic resonance study of metal ion complexation. Proc. R. Soc. London, Ser. A 2010, 466 (2117), 1489–1513.
(31) Ottaviani, M. F.; Cangiotti, M.; Fattori, A.; Coppola, C.; Posocco, P.; Laurini, E.; Liu, X.; Liu, C.; Fermeglia, M.; Peng, L.; Pricl, S. Copper(ii) binding to flexible triethanolamine-core PAMAM dendrimers: a combined experimental/in silico approach. Phys. Chem. Chem. Phys. 2014, 16 (2), 685–694.
(32) García-Gallego, S.; Cangiotti, M.; Fiorani, L.; Fattori, A.; Muñoz-Fernández, M. a. Á.; Gomez, R.; Ottaviani, M. F.; de la Mata, F. J. Anionic sulfonated and carboxylated PPI dendrimers with

the EDA core: synthesis and characterization of selective metal complexing agents. Dalton Trans. 2013, 42 (16), 5874−5889.
(33) Tang, Y.-H.; Cangiotti, M.; Kao, C.-L.; Ottaviani, M. F. EPR Characterization of Copper(II) Complexes of PAMAM-Py Dendrimers for Biocatalysis in the Absence and Presence of Reducing Agents and a Spin Trap. J. Phys. Chem. B 2017, 121 (46), 10498−10507.
(34) Fox, L. J.; Richardson, R. M.; Briscoe, W. H. PAMAM dendrimer - cell membrane interactions. Adv. Colloid Interface Sci. 2018, 257, 1− 18.
(35) Seib, F. P.; Jones, A. T.; Duncan, R. Comparison of the endocytic properties of linear and branched PEIs, and cationic PAMAM dendrimers in B16f10 melanoma cells. J. Controlled Release 2007, 117 (3), 291−300.
(36) Kummar, S.; Gutierrez, M.; Doroshow, J. H.; Murgo, A. J. Drugdevelopment in oncology: classical cytotoxics and molecularly targetedagents. Br. J. Clin. Pharmacol. 2006, 62 (1), 15−26.
(37) Krasheninina, O.; Apartsin, E.; Fuentes, E.; Szulc, A.; Ionov, M.;Venyaminova, A.; Shcharbin, D.; De la Mata, F.; Bryszewska, M.; Gomez, R. Complexes of Pro-Apoptotic siRNAs and Carbosilane Dendrimers: Formation and Effect on Cancer Cells. Pharmaceutics 2019, 11 (1), 25.
(38) Zhang, Y.; Zhang, L.; Gao, J.; Wen, L. Pro-Death or Pro-Survival: Contrasting Paradigms on Nanomaterial-Induced Autophagy and Exploitations for Cancer Therapy. Acc. Chem. Res. 2019, 52 (11), 3164−3176.
(39) Ditsworth, D.; Zong, W. X.; Thompson, C. B. Activation of poly(ADP)-ribose polymerase (PARP-1) induces release of the proinflammatory mediator HMGB1 from the nucleus. J. Biol. Chem. 2007, 282 (24), 17845−54.
(40) Campisi, J.; d'Adda di Fagagna, F. Cellular senescence: when bad things happen to good cells. Nat. Rev. Mol. Cell Biol. 2007, 8 (9), 729− 740.
(41) Jäger, R.; Fearnhead, H. O. ''Dead Cells Talking'': The Silent Form of Cell Death Is Not so Quiet. Biochem. Res. Int. 2012, 2012, 453838−453838.
(42) Touil, Y.; Igoudjil, W.; Corvaisier, M.; Dessein, A. F.; Vandomme, J.; Monte, D.; Stechly, L.; Skrypek, N.; Langlois, C.; Grard, G.; Millet, G.; Leteurtre, E.; Dumont, P.; Truant, S.; Pruvot, F. R.; Hebbar, M.; Fan, F.; Ellis, L. M.; Formstecher, P.; Van Seuningen, I.; Gespach, C.; Polakowska, R.; Huet, G. Colon cancer cells escape 5FU chemotherapy-induced cell death by entering stemness and quiescence associated with the c-Yes/YAP axis. Clin. Cancer Res. 2014, 20 (4), 837−46.
(43) Janaszewska, A.; Gorzkiewicz, M.; Ficker, M.; Petersen, J. F.; Paolucci, V.; Christensen, J. B.; Klajnert-Maculewicz, B. Pyrrolidone Modification Prevents PAMAM Dendrimers from Activation of Pro- Inflammatory Signaling Pathways in Human Monocytes. Mol. Pharmaceutics 2018, 15 (1), 12−20.
(44) Zorova, L. D.; Popkov, V. A.; Plotnikov, E. Y.; Silachev, D. N.; Pevzner, I. B.; Jankauskas, S. S.; Babenko, V. A.; Zorov, S. D.; Balakireva, A. V.; Juhaszova, M.; Sollott, S. J.; Zorov, D. B. Mitochondrial membrane potential. Anal. Biochem. 2018, 552, 50−59. (45) Battogtokh, G.; Choi, Y. S.; Kang, D. S.; Park, S. J.; Shim, M. S.; Huh, K. M.; Cho, Y.-Y.; Lee, J. Y.; Lee, H. S.; Kang, H. C. Mitochondria- targeting drug conjugates for cytotoxic, anti-oxidizing and sensing purposes: current strategies and future perspectives. Acta Pharm. Sin. B 2018, 8, 862.
(46) Cesarini, E.; Cerioni, L.; Canonico, B.; Di Sario, G.; Guidarelli, A.; Lattanzi, D.; Savelli, D.; Guescini, M.; Nasoni, M. G.; Bigini, N.; Cuppini, R.; Stocchi, V.; Ambrogini, P.; Papa, S.; Luchetti, F. Melatonin protects hippocampal HT22 cells from the effects of serum deprivation specifically targeting mitochondria. PLoS One 2018, 13 (8), e0203001.
(47) Zorov, D. B.; Juhaszova, M.; Sollott, S. J. Mitochondrial ROS- induced ROS release: an update and review. Biochim. Biophys. Acta, Bioenerg. 2006, 1757 (5−6), 509−17.

(48) Zhang, H.; Chang, Z.; Mehmood, K.; Abbas, R. Z.; Nabi, F.; Rehman, M. U.; Wu, X.; Tian, X.; Yuan, X.; Li, Z.; Zhou, D. Nano Copper Induces Apoptosis in PK-15 Cells via a Mitochondria-Mediated Pathway. Biol. Trace Elem. Res. 2018, 181 (1), 62−70.
(49) Blecha, J.; Novais, S. M.; Rohlenova, K.; Novotna, E.; Lettlova, S.; Schmitt, S.; Zischka, H.; Neuzil, J.; Rohlena, J. Antioxidant defense in quiescent cells determines selectivity of electron transport chain inhibition-induced cell death. Free Radical Biol. Med. 2017, 112, 253−266.
(50) Morganti, C.; Bonora, M.; Ito, K.; Ito, K. Electron transport chain complex II sustains high mitochondrial membrane potential in hematopoietic stem and progenitor cells. Stem Cell Res. 2019, 40,101573.
(51) Zischka, H.; Einer, C. Mitochondrial copper homeostasis and its derailment in Wilson disease. Int. Int. J. Biochem. Cell Biol. 2018, 102, 71−75.
(52) Michlewska, S.; Ionov, M.; Shcharbin, D.; Maroto-Díaz, M.; Gomez, R. R.; de la Mata, F. J.; Bryszewska, M. Ruthenium metallodendrimers with anticancer potential in an acute promyelocytic leukemia cell line (HL60). Eur. Polym. J. 2017, 87, 39−47.
(53) Li, Y.; Ju, D. The Role of Autophagy in Nanoparticles-Induced Toxicity and Its Related Cellular and Molecular Mechanisms. Adv. Exp. Med. Biol. 2018, 1048, 71−84.
(54) Fulda, S. Autophagy in Cancer Therapy. Front. Oncol. 2017, 7, 128−128.
(55) McLeod, I. X.; He, Y. Roles of autophagy in lymphocytes: reflections and directions. Cell. Mol. Immunol. 2010, 7 (2), 104−107.
(56) Li, Y.; Zhu, H.; Wang, S.; Qian, X.; Fan, J.; Wang, Z.; Song, P.; Zhang, X.; Lu, W.; Ju, D. Interplay of Oxidative Stress and Autophagy in PAMAM Dendrimers-Induced Neuronal Cell Death. Theranostics 2015, 5 (12), 1363−77.
(57) Li, F.; Li, Z.; Jin, X.; Liu, Y.; Zhang, P.; Li, P.; Shen, Z.; Wu, A.; Chen, W.; Li, Q. Ultra-small gadolinium oxide nanocrystal sensitization of non-small-cell lung cancer cells toward X-ray irradiation by promoting cytostatic autophagy. Int. J. Nanomed. 2019, 14, 2415−2431.
(58) Thomas, T. P.; Majoros, I.; Kotlyar, A.; Mullen, D.; Banaszak Holl, M. M.; Baker, J. R. Cationic poly(amidoamine) dendrimer induces lysosomal apoptotic pathway at therapeutically relevant concentrations. Biomacromolecules 2009, 10 (12), 3207−3214.
(59) Stern, S. T.; Adiseshaiah, P. P.; Crist, R. M. Autophagy and lysosomal dysfunction as emerging mechanisms of nanomaterial toxicity. Part. Fibre Toxicol. 2012, 9, 20−20.

TABLE OF CONTENTS GRAPHIC